# Supporting Information

## MXene-Supported Cu-Ag Nanohybrids for Electrochemical Nitrate and Nitrite Detection in Alkaline Media

Vishwanath Ankalgi[a], Mohammed Arkham Belgami[a], Bhakti Kulkarni[a], Sang Mun Jeong[b*], Chandra Sekhar Rout[a*]

[a]*Centre for Nano and Material Sciences, Jain University, Ramanagara, Bangalore 562112, India.*
[b]*Department of Chemical Engineering, Chungbuk National University, Cheongju, Chungbuk 28644, Republic of Korea.*

Corresponding Authors: r.chandrasekhar@jainuniversity.ac.in (C. S. Rout)
smjeong@chungbuk.ac.kr (S. M. Jeong)

## Experimental Section

### *Electrochemical detection of Analyte*

This study observed that the careful selection of the electrolyte (*An ionic medium that enables electrochemical reactions by providing both electroactive species and background ions for charge transport and conductivity.*), optimization of pH, adjustment of the mass loading ratio, and use of the surface charge collectively contributed to enhanced nitrate removal efficiency. Optimization of the pH was further undertaken to elucidate the probable sensing mechanisms operative within the system. Among various electrolytes tested, 0.1 M $Na_2SO_4$ at pH 11.0 was identified as the most suitable supporting electrolyte (*An inert ionic species added to maintain high ionic strength, minimize ion migration, and stabilize the electric field during electrochemical measurements, without participating in redox reactions.*) for subsequent electrochemical processes. Corresponding to the sequential reduction of nitrate ($NO_3^-$) to nitrite ($NO_2^-$) and subsequently to ammonia ($NH_3$). The complete reaction suggests a one-step multidetection type device. The equimolar ratio of both Ag nanoparticles was involved in $NO_3^-$ reduction at -0.89 V of overpotential, and Cu nanoparticles reduced the $NO_2^-$ at -1.15 V overpotential, respectively. Given that the pH of most soil environments tends to be alkaline, the sensor's good performance at higher pH levels makes it well-suited for detecting $NO_3^-$ in soil. In this work, both aqueous and soil samples were analyzed to evaluate the selectivity and sensitivity of the Ag- and Cu-modified $Ti_3C_2T_x$ (denoted as 5TCX-AgCu) towards $NO_3^-$ detection. Additionally, Zobell's solution (consisting of 0.1 M KCl with an equimolar mixture of potassium ferrocyanide and potassium ferricyanide) was employed to conduct film characterization studies and to determine the oxidation-reduction potential (ORP) of the unmodified and modified electrode substrates. Film characterization studies were further carried out on the screen-printed carbon electrode (SPCE) substrate using Zobell's solution, with cyclic voltammetry (CV) measurements performed within a potential window of -0.6 to +0.6 V. Electrochemical impedance spectroscopy was utilized to extract key parameters, including solution resistance ($R_s$) and charge transfer resistance ($R_{ct}$), as well as to analyze ion diffusion behavior through Warburg impedance modeling. Based on the results obtained from film studies and impedance analyses, the SPCE substrate was found to exhibit excellent electrochemical properties, thereby confirming its suitability for $NO_3^-$ and $NO_2^-$ sensing applications. Electrochemical characterizations, including CV, square wave voltammetry (SWV), electrochemical impedance spectroscopy (EIS), and chronoamperometry (CA), were

systematically conducted to achieve precise calibration and thorough evaluation of the 5TCX-AgCu as a modified electrode for electrochemical sensing applications. For $NO_3^-$ and $NO_2^-$ detection, a potential window of 0 to -1.3 V was employed during CV and SWV measurements. Different concentrations of $NO_3^-$ and $NO_2^-$ were successively introduced into the electrolyte system as the modified electrode was immersed, allowing for the assessment of sensor performance across a range of analyte levels.

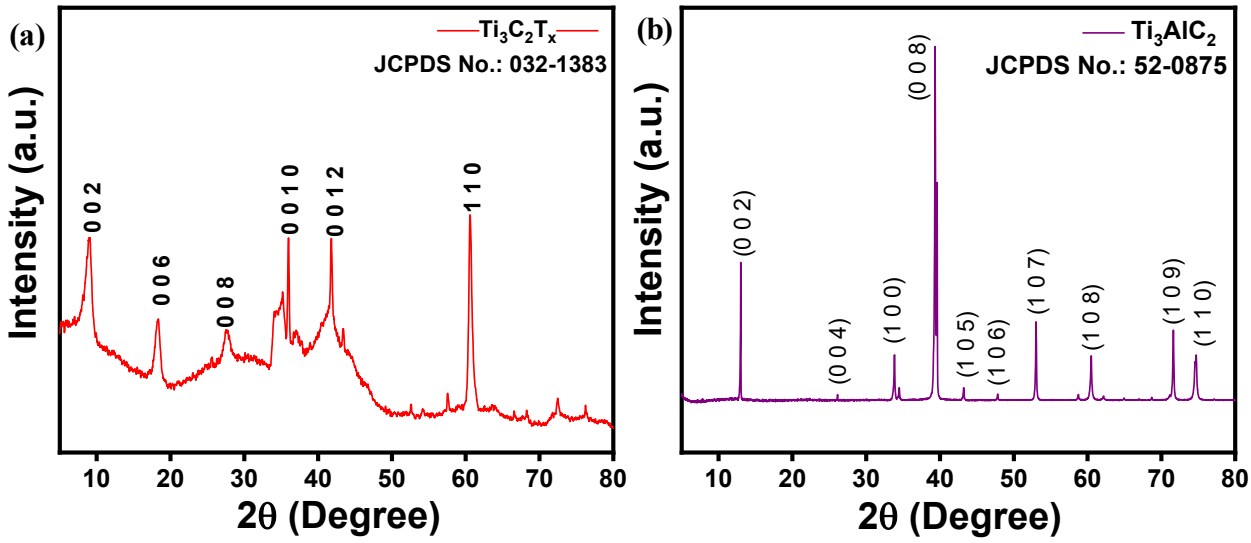


**Figure S1:** XRD analysis of (a) $Ti_3C_2T_x$, (b) $Ti_3AlC_2$.

**Table S1:** Comparison table for particle size.

| Technique | Average Size (nm) | Measurement Basis |
|---|---|---|
| **XRD** | **6-15 nm** | **Crystallite size via Scherrer equation** |
| **SEM** | **12-30 nm** | **Surface morphology** |
| **TEM** | **3-5 nm** | **Individual particles** |

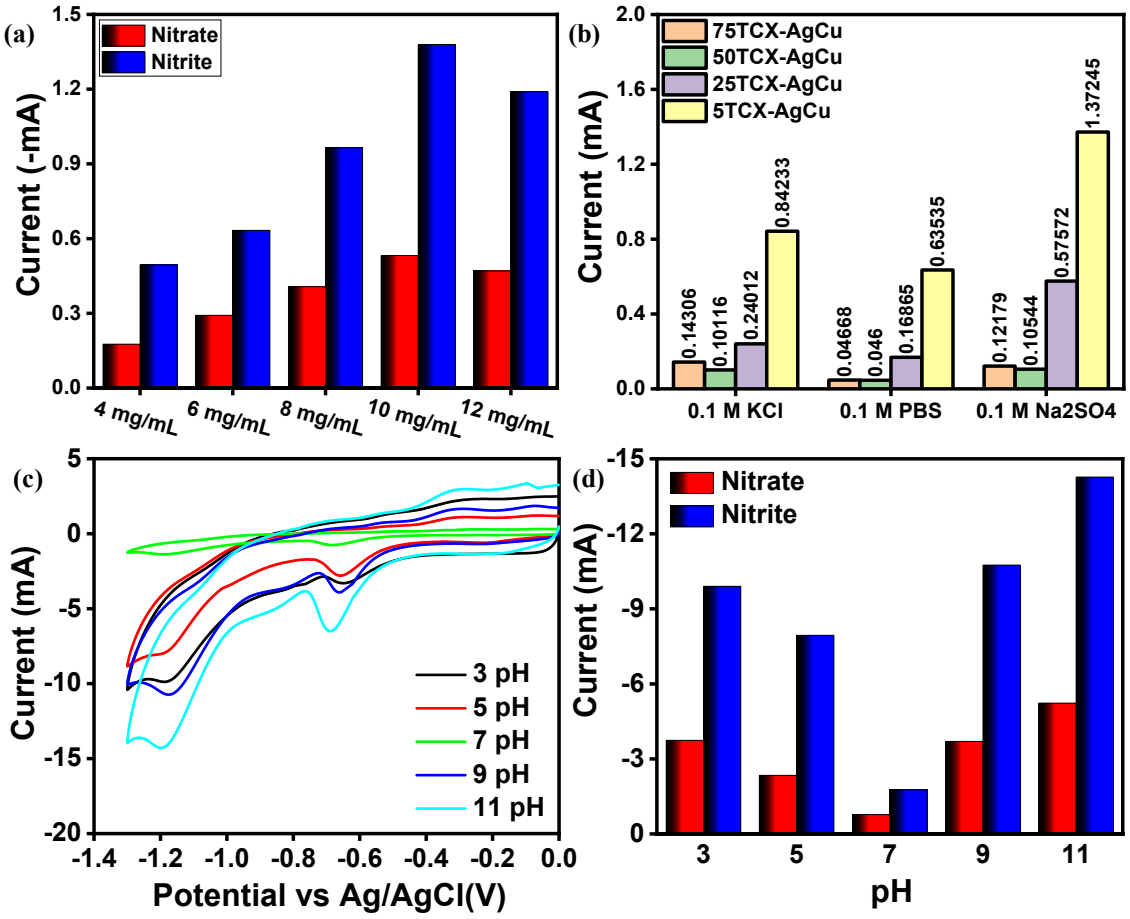


**Figure S2:** (a) Mass loading studies done in 0.1M $Na_2SO_4$ (pH 7.0) for 5TCX-AgCu, (b) Bar graph represents comparative CV responses of 20 mM $NO_3^-$ detection in different electrolytes (pH 7.0); (c) Evaluation of pH-dependent electrochemical response of the 5TCX-AgCu composite, (d) Bar graph representation of pH graph.

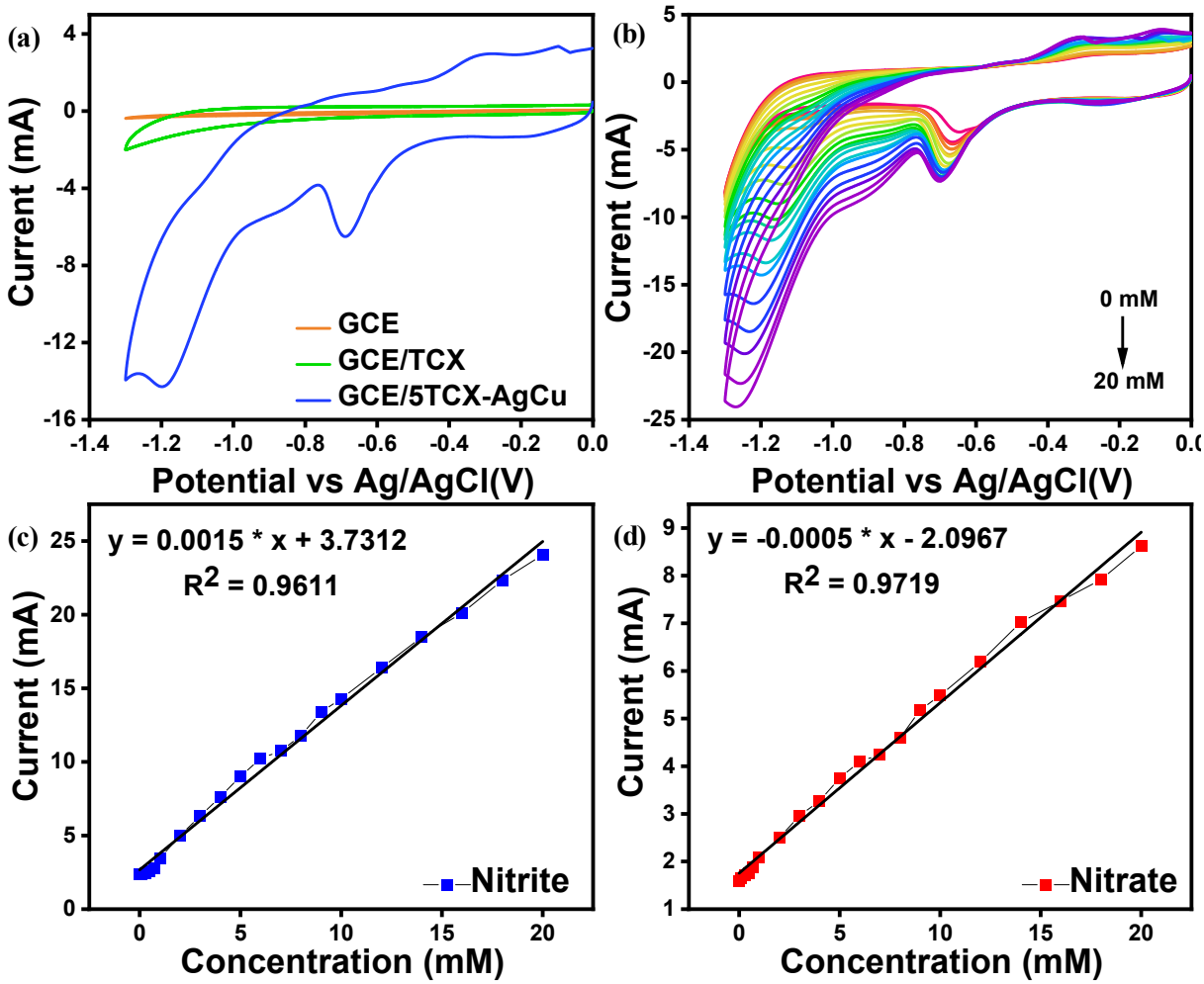


**Figure S3:** (a) CVs for GCE, GCE/TCX, and GCE/5TCX-AgCu were recorded in 0.1 M $Na_2SO_4$ (pH 11) containing 10 mM $NO_3^-$; (b) CV responses of 5TCX-AgCu were evaluated in 0.1 M $Na_2SO_4$ (pH 11) over a $NO_3^-$ concentration range of (0, 0.1, 0.3, 0.5, 0.7, 1, 2, 3, 4, 5, 6, 7, 8, 9, 10, 15, 20 mM); Corresponding calibration plots were constructed for (c) $NO_2^-$ and (d) $NO_3^-$ detection.

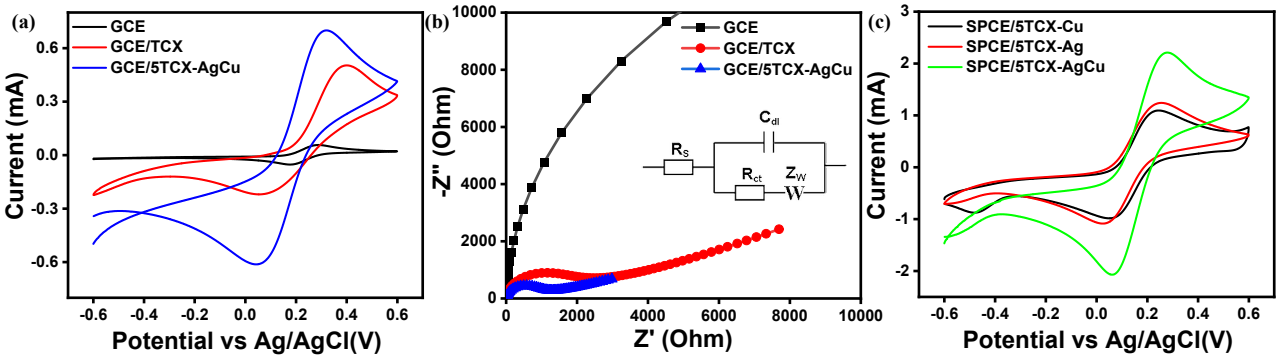


**Figure S4:** (a) CV comparison of bare GCE, GCE/TCX, and GCE/5TCX-AgCu electrodes; (b) EIS comparison in Zobell's solution for oxidation–reduction potential (ORP) assessment, (c) CV comparison of SPCE/TCX-Ag, SPCE/TCX-Cu, and SPCE/TCX-AgCu in Zobell's solution.

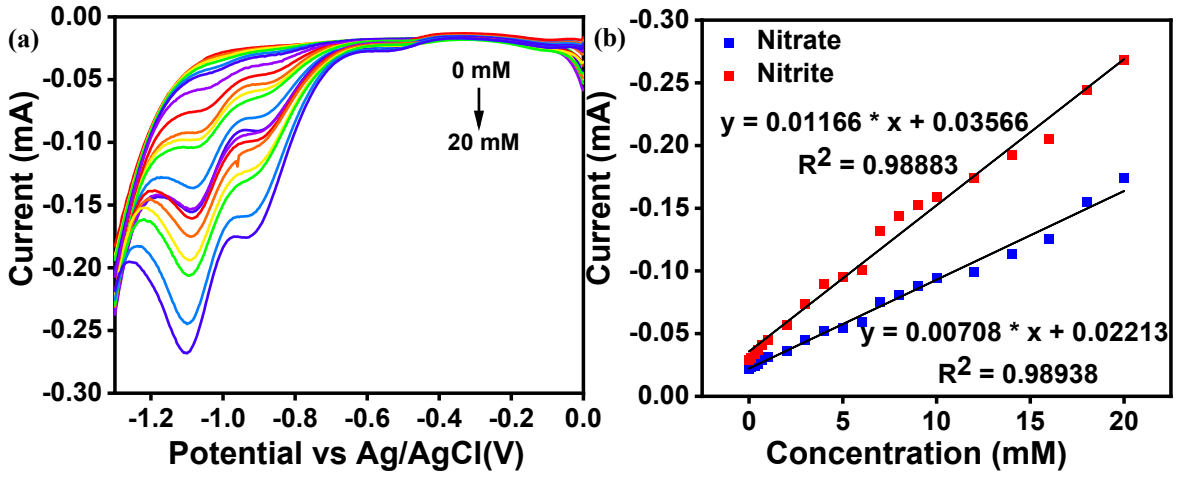


**Figure S5:** (a) SWV responses of the 5TCX-AgCu in 0.1M $Na_2SO_4$ (pH 11.0); (b) Calibration plot of $NO_3^-$ and $NO_2^-$.

**Table S2:** Comparison studies reported using different modified electrodes for electrochemical $NO_3^-$ sensing.

| Electrode & Method Materials | Electrolyte & pH | Linear Range (µM) | Limit of Detection (µM) | Sensitivity (µA µM$^{-1}$ cm$^{-2}$) | Ref. |
|---|---|---|---|---|---|

| | | | | | | |
|---|---|---|---|---|---|---|
| PPy/Ag | CV | $Na_2SO_4$, pH 3 | 1-$10^4$ | 5 | NR | [31] |
| NPs/GCE | DPV | $Na_2SO_4$, pH 7 | 1-$10^5$ | 2 | 2.317 | [32] |
| Ag NPs/AuE | CV | Sea water, pH 5 | 10-$10^4$ | 10 | NR | [33] |
| | SWV | NaCl, pH 7 | 0.39-50 | 0.39 | 0.1057 | [34] |
| Pd-Au NPs composite | LSV | Water, pH 7.2 | 16-242 | 1.19 | 0.29 | [35] |
| Gr/CuE | Am | NaOH, pH 12 | 9-940 | 10 | 0.173 | [36] |
| Porous Cu-Ni alloy | Am | $Na_2SO_4$, pH 13 | 20-$10^3$ | 2, 7 | 10.9, 5.1 | [37] |
| Rh-modified Cu porous layer | Am | $Na_2SO_4$, pH 7 and 13 | 20-$10^3$ | 20, 6 | 12.3, 6 | [37] |
| Macroporous Ag film/ITO | SWV | NaOH, pH 14 | 20-$5\times10^3$ | NR | 0.093 | [38] |
| **5TCX-AgCu/SPCE** | **SWV** | **$Na_2SO_4$, pH 11** | **10-$10^5$** | **5.2** | **120.75** | **Present Work** |

**CV:** Cyclic Voltammetry, **SWV:** Square wave Voltammetry, **DPV:** Differential Pulse Voltammetry, **LSV:** Linear Sweep Voltammetry, **Am:** Amperometric, **PPy:** Polypyrrole, **NP:** Nanoparticle, **TCX:** $Ti_3C_2T_x$, **Pd:** Palladium, **Au:** Gold, **Cu:** Copper, **Ni:** Nickel, **Ag:** Silver, **Rh:** Rhodium, **Gr:** Graphite, **GCE:** Glassy carbon electrode, **SPCE:** Screen printed carbon electrode, **AuE:** Gold electrode, **CuE:** Cu electrode.

**Table S3:** Comparison studies reported using different modified electrodes for electrochemical $NO_2^-$ sensing by reduction.

| **Electrode & Materials** | **Method** | **Electrolyte & pH** | **Linear Range (µM)** | **Limit of Detection (µM)** | **Sensitivity (µA $µM^{-1}$ $cm^{-2}$)** | **Ref.** |
|---|---|---|---|---|---|---|
| Bare copper | DPV | $Na_2SO_4$, pH 2 | 0.17-100 | 0.17 | NR | [39] |
| POM/GCE | Am | $Li_2SO_4$, pH 1.2 | 0.1-20000 | 0.1 | 385.94 | [40] |
| BDD | DPV | PBS, pH 6 | 10-8000 | 18 | NR | [41] |

| | | | | | | |
|---|---|---|---|---|---|---|
| PB/CPE | Am | PBS, pH 1 | 25-1000 | 9 | NR | [42] |
| Cu/MWCNT/ RGO/GCE | SWV | $Na_2SO_4$, pH 3 | 0.1-75 | 0.03 | NR | [11] |
| Rh-complex/MW CNT/GCE | Am | PBS, pH 2 | 0.25-10 | 0.08 | 60 | [43] |
| PtNP/TH/M WCNT | CV | NaOH, pH 7 | 0.5–150 | 0.2 | 0.05 | [44] |
| **5TCX-AgCu/SPCE** | **SWV** | **$Na_2SO_4$, pH 11** | **1-$10^3$** | **0.031** | **898.12** | **Present work** |

**SWV:** Square Wave Voltammetry, **DPV:** Differential Pulse Voltammetry, **Am:** Amperometric, **POM:** Polyoxometalates, **BDD:** Boron-Doped Diamond, **PB:** Prussian Blue, **CPE:** Carbon Paste Electrode, **Cu:** Copper, **MWCNT:** Multiwalled Carbon Nanotubes, **RGO:** Reduced Graphene Oxide, **GCE:** Glassy Carbon Electrode, **Rh:** Rhodium, **PtNP:** Platinum Nanoparticle, **TH:** Thionine, **TCX:** $Ti_3C_2T_x$, **Ag:** Silver, **Cu:** Copper, **SPCE:** Screen Printed Carbon Electrode.

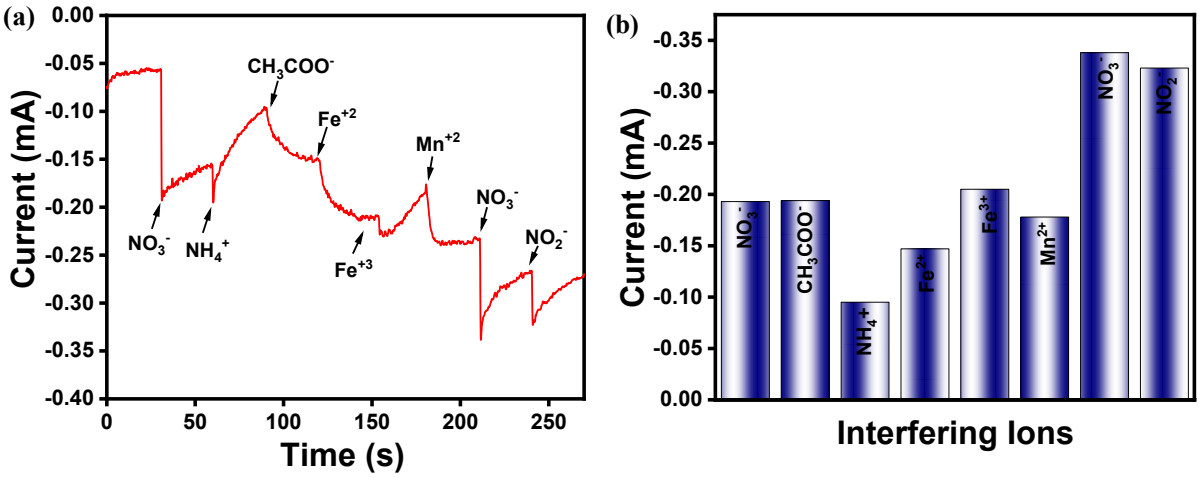


**Figure S6:** Interference study for the 5TCX-AgCu, (a) Potentiostatic method representation, (b) Bar graph representation.

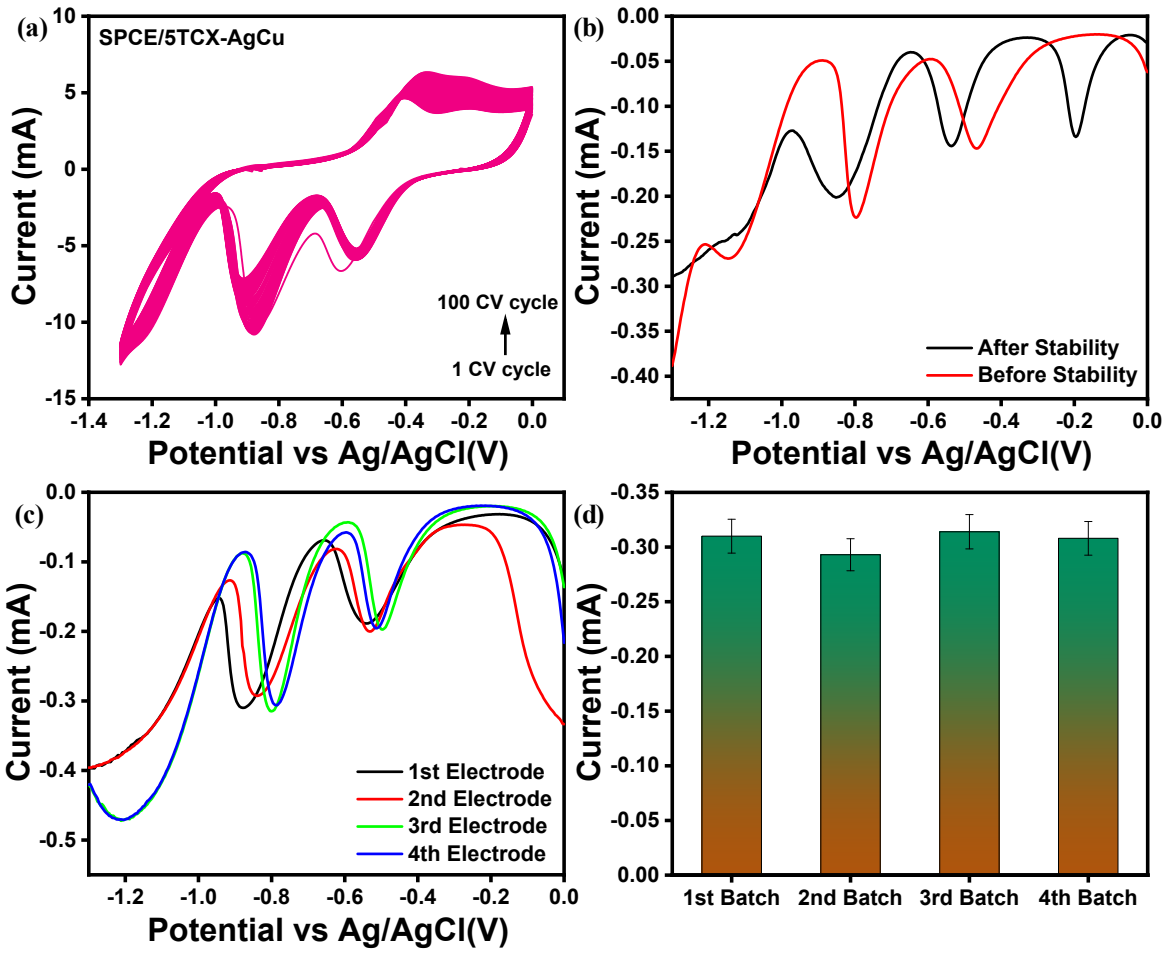


**Figure S7:** (a) CV performed over 100 cycles in 0.1 M $Na_2SO_4$ (pH 11.0) containing 20 mM $NO_3^-$ demonstrating electrochemical stability. (b) SWV was recorded before and after the stability test under the same conditions. (c) Evaluation of the reproducibility of SPCE/5TCX-AgCu electrodes in 0.1 M $Na_2SO_4$ (pH 11.0) using four independently fabricated sensors. (d) Bar graph representation of the same.

**Table S4:** Real sample analysis for the 5TCX-AgCu.

| Samples | Spiked (mM) | Found (mM) | Recovery % |
|---|---|---|---|
| Soil water | 16 | 13.6 | 85 |
| | 18 | 15.9 | 82.7 |

| | | | |
|---|---|---|---|
| | **20** | **17.5** | **87.5** |
| **Lake water** | **16** | **15** | **93.75** |
| | **18** | **17.2** | **95.5** |
| | **20** | **18.6** | **93** |
| **River water** | **16** | **14.9** | **93.12** |
| | **18** | **17** | **94.44** |
| | **20** | **18.5** | **92.5** |

**References:**


11 H. Bagheri, A. Hajian, M. Rezaei and A. Shirzadmehr, *Journal of Hazardous Materials*, 2017, **324**, 762–772.

31 M. Atmeh and B. E. Alcock-Earley, *J Appl Electrochem*, 2011, **41**, 1341–1347.

32 G. Khadigeh, .

33 K. Fajerwerg, V. Ynam, B. Chaudret, V. Garçon, D. Thouron and M. Comtat, *Electrochemistry Communications*, 2010, **12**, 1439–1441.

34 D. Chen Legrand, C. Barus and V. Garçon, *Electroanalysis*, 2017, **29**, 2882–2887.

35 S. Zhao, J. Tong, Y. Li, J. Sun, C. Bian and S. Xia, *Micromachines*, 2019, **10**, 223.

36 T. Öznülüer, B. Özdurak and H. Öztürk Doğan, *Journal of Electroanalytical Chemistry*, 2013, **699**, 1–5.

37 N. Comisso, S. Cattarin, P. Guerriero, L. Mattarozzi, M. Musiani, L. Vázquez-Gómez and E. Verlato, *J Solid State Electrochem*, 2016, **20**, 1139–1148.

38 M.-C. Tsai, D.-X. Zhuang and P.-Y. Chen, *Electrochimica Acta*, 2010, **55**, 1019–1027.

39 S. M. Shariar and T. Hinoue, *ANAL. SCI.*, 2010, **26**, 1173–1179.

40 M. Ammam, B. Keita, L. Nadjo and J. Fransaer, *Talanta*, 2010, **80**, 2132–2140.

41 Z. Zhang, G. Ogata, K. Asai, T. Yamamoto and Y. Einaga, *ACS Sens.*, 2023, **8**, 4245–4252.

42 L. A. Pradela-Filho, B. C. Oliveira, R. M. Takeuchi and A. L. Santos, *Electrochimica Acta*, 2015, **180**, 939–946.

43 R. Hallaj, A. Salimi, B. Kavosi and G. Mansouri, *Sensors and Actuators B: Chemical*, 2016, **233**, 107–119.

44 R. Yu, L. Wang, Q. Xie and S. Yao, *Electroanalysis*, 2010, **22**, 2856–2861.